# Theoretical Study of the 1,3-Dipolar Cycloaddition Reactions of Azomethine Ylides. A DFT Study of Reaction between Trifluoromethyl Thiomethyl Azomethine Ylide and Acronitrile

Luis R. Domingo†

*Departamento de Química Orgánica, Universidad de Valencia, Dr. Moliner 50, 46100 Burjassot, Valencia, Spain*

*Received November 13, 1998*

The molecular mechanism for the 1,3-dipolar cycloaddition of trifluoromethyl thiomethyl azomethine ylide with acronitrile has been characterized using density functional theory methods with the B3LYP functional and the 6-31G* and 6-31+G** basis sets. Relative rates, regioselectivity and *endo* stereoselectivity are analyzed and discussed. Analysis of the results on the different reaction pathways shows that the reaction takes place along a concerted mechanism, where the two carbon−carbon forming bonds are dissymmetrically formed. This cycloaddition presents a total regioselectivity and *endo* stereoselectivity, due to a strong polarization of both dissymmetric dipole and dipolarophile reactants, and a favorable hyperconjugative delocalization that appears along the *endo* approach. Density functional calculations at the B3LYP/6-31G* theory level provide data on transition-state energies for this 1,3-dipolar cycloaddition in full agreement with the stereochemical outcome.

## Introduction

The cycloaddition of a 1,3-dipolar species to an alkene for the synthesis of five-membered rings is a classic reaction in organic chemistry. The 1,3-dipolar cycloaddition (1,3-DC) reactions are used for the preparation of molecules of fundamental importance for both academia and industry.[1]

The development of 1,3-DC reactions has in recent years entered a new stage, as control of the stereochemistry in the addition step is now the major challenge. The stereochemistry challenge is to control the regio-, diastereo-, and enantioselectivity of the 1,3-DC reactions. The stereochemistry of these reactions can be controlled by either choosing the appropriate substrates or controlling the reaction by a metal complex acting as catalyst.[1]

Azomethine ylides, 2-azaallyl anions, which add to a variety of olefins to form pyrrolidine derivatives, have been used as 1,3-dipoles.[2] Azomethine ylides are unstable species which have to be prepared in situ. Recently, Viehe et al.[3] have described the 1,3-DC reaction between a trifluoromethyl thiomethyl azomethine ylide prepared by deprotonation of the trifluoromethyl thioamidium salt **1**, with several dipolarophiles containing electron-withdrawing substituents to give a mixture of diastereomeric pyrrolidines (see Scheme 1). These 1,3-DC reactions take place with a total regioselectivity and *endo* stereoselectivity. Thus, for the reaction between this azomethine ylide and acronitrile, two diastereomeric pyrrolidines are obtained in a 96:4 ratio.

Several theoretical works have been devoted to the study of 1,3-DC reactions; however, this cycloaddition form has not received the same amount of attention as its counterpart, the Diels−Alder reaction.[4] In addition, few of them have been devoted to the study of azomethine ylides as dipoles in 1,3-DC reactions.

**Scheme 1**

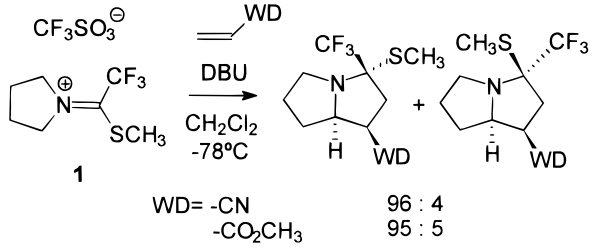


Annunziata et al.[5] studied the 1,3-DC reaction of the simplest azomethine ylide ($CH_2NHCH_2$), **2**, with ethylene using PM3 and ab initio calculations. These authors proposed a concerted mechanism to find a symmetric transition structure (TS) at the RHF/3-21G level, with a length of the two bonds being formed of 2.479 Å (see Figure 1). This large bond length indicates that this TS is remarkably early.[5]

On the other hand, Kanemasa et al.[6] proposed a stepwise mechanism for the reaction of the lithium (*Z*)-enolate derived from *N*-alkylideneglycinate with α,*β*-unsaturated esters by theoretical calculations using MNDO and PM3 procedures. The initial step consists of an anti-selected carbon−carbon bond formation by a Michael addition of the ylide to the conjugated position of the α,*β*-unsaturated ester (Scheme 2). Recently, Cossío et al.[7] studied the 1,3-DC reaction of several N-metaled azomethine ylides with nitroalkenes, using PM3 procedures. These authors also proposed a stepwise mecha-

† E-mail: domingo@utopia.uv.es.

(1) Gothelf, K. V.; Jorgensen, K. A. *Chem. Rev.* **1998**, *98*, 863.
(2) Carruthers, W. *Some Modern Methods of Organic Synthesis*, 2nd ed.; Cambridge University Press: Cambridge, 1978.
(3) Laduron, F.; Ates, C.; Viehe, H. G. *Tetrahedron Lett.* **1996**, *37*, 5515.
(4) (a) Sauer, J.; Sustmann, R. *Angew. Chem., Int. Ed. Engl.* **1980**, *19*, 778. (b) Houk, K. N.; González, J.; Li, Y. *Acc. Chem. Res.* **1995**, *28*, 81.
(5) Annunziata, R.; Benaglia, M.; Cinquini, M.; Raimondi, L. *Tetrahedron Lett.* **1993**, *49*, 8629.
(6) Tatsukawa, A.; Hawatake, K.; Kanemasa, S.; Rudzinski, J. M. *J. Chem. Soc., Perkin Trans. 2* **1994**, 2525.
(7) Ayerbe, M.; Arrieta, A.; Cossío, F. P. *J. Org. Chem.* **1998**, *63*, 1795.

10.1021/jo9822683 CCC: $18.00 
Published on Web 05/04/1999

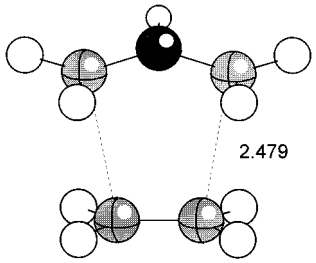


**Figure 1.** HF/3-21G transition structure for the 1,3-DC reaction between the azomethine ylide **2** and ethene.

**Scheme 2**

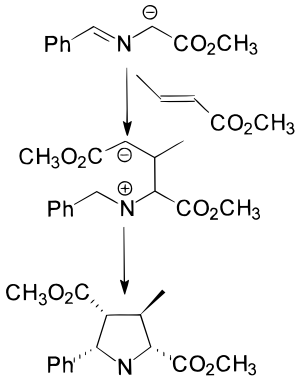


nism due to the high electron-withdrawing character of the nitroalkene, which behaves as a Michael acceptor rather than a dipolarophile. The stereochemical outcome of these reactions depends on the hardness of metal. The nitro group shows more affinity for the hardest metal (lithium relative to silver) promoting *endo* selectivity.

The reaction of the 5-(*R*)-menthyloxy-2(5*H*)-furanone with a *N*-benzyl-α-ethoxycarbonyl-substituted ylide was also investigated by frontier molecular orbital (FMO) analysis using AM1 calculations.[8] On the basis of this analysis it was supposed that the α-ester carbon atom of the ethoxycarbonyl azomethine ylide reacts preferentially with the *β*-enone carbon atom of the alkene, and the reaction is $HOMO_{dipole}$−$LUMO_{alkene}$ controlled.

Our research program has long maintained an interest in the study of the molecular mechanism of cycloaddition reactions using quantum chemical procedures, to provide the regio- and stereochemical outcomes and to shed light on the mechanistic details of these important reactions. In the present work, a density functional theory (DFT) study for the 1,3-DC reaction between the trifluoromethyl thiomethyl azomethine ylide and acronitrile reported by Viehe et al.[3] is carried out in order to understand the mechanistic details and to prove the ability of these theoretical tools to shed light on this sort of 1,3-DC reaction. Our main purpose is the study of the molecular mechanism of this reaction in order to explain the stereochemical outcomes.

## Computing Methods

In recent years theoretical methods based on density functional theory[9] have emerged as an alternative to traditional ab initio methods in the study of structure and reactivity of chemical systems. Diels−Alder reactions and related reactions have been the object of several density functional studies showing that functionals that include gradient corrections and hybrid functionals, such as B3LYP, together with the 6-31G* basis set, lead to potential energy barriers in good agreement with the experimental results.[10] Thus, in the present study geometrical optimizations of the stationary points along the potential energy surface (PES) were carried out using the gradient-corrected functional of Becke, and Lee, Yang, and Parr (B3LYP)[11] for exchange and correlation, with the standard 6-31G* basis set.[12] Since it was expected that some negative charge can be located in any stationary point, the 6-31+G** basis set was also used because of its superior ability to accommodate negative charges.

The stationary points were characterized by frequency calculations in order to verify that minima and transition structures have zero and one imaginary frequency, respectively. The optimizations were carried out using the Berny analytical gradient optimization method.[13] The transition vectors (TV),[14] i.e., the eigenvector associated with the unique negative eigenvalue of the force constants matrix, have been characterized. Optimized geometries of all the structures are available from the author.

Due to the presence of weak van der Waals molecular complexes which are likely formed at the early stages of the reaction, counterpoise estimates of basis set superposition error (BSSE)[15] were made by performing calculations on dipole and dipolarophile reactants including basis functions from the other reactant, in the molecular complex geometries.

The electronic structures of stationary points were analyzed by the natural bond orbital (NBO) method.[16] All calculations were carried out with the Gaussian 94 suite of programs.[17]

## Results and Discussions

**I. Theoretical Study of the Molecular Structure of the Azomethine Ylides R1 and R2.** As stated in the Introduction, the azomethine ylides are unstable species that must be prepared in situ. The trifluoromethyl thiomethyl azomethine ylide is prepared by proton

(8) Rispens, M. T.; Keller, E.; Lange, B. de; Zijlstra, R. W. J.; Feringa, B. L. *Tetrahedron Asymmetry* **1994**, *5*, 607.

(9) (a) Parr, R. G.; Yang, W. *Density Functional Theory of Atoms and Molecules*; Oxford University Press: New York, 1989. (b) Ziegler, T. *Chem. Rev.* **1991**, *91*, 651.

(10) (a) Stanton, R. V.; Merz, K. M. *J. Chem. Phys.* **1994**, *100*, 434. (b) Carpenter, J. E.; Sosa, C. P. *THEOCHEM* **1994**, *311*, 325. (c) Baker, J.; Muir, M.; Andzelm, J. *J. Chem. Phys.* **1995**, *102*, 2036. (d) Jursic, B.; Zdravkovski, Z. *J. Chem. Soc., Perkin Trans 2* **1995**, 1223. (e) Goldstein, E.; Beno, B.; Houk, K. N. *J. Am. Chem. Soc.* **1996**, *118*, 6036. (f) Branchadell, V. *Int. J. Quantum Chem.* **1997**, *61*, 381. (g) Sbai, A.; Branchadell, V.; Ortuño, R. M.; Oliva, A. *J. Org. Chem.* **1997**, *62*, 3049. (h) Branchadell, V.; Font, J.; Moglioni, A. G.; Ochoa de Echaguen, C.; Oliva, A.; Ortuno, R. M.; Veciana, J.; Vidal Gancedo, J. *J. Am. Chem. Soc.* **1997**, *119*, 9992. (i) García, J. I.; Martínez-Merino, V.; Mayoral, J. A.; Salvatella, L. *J. Am. Chem. Soc.* **1998**, *120*, 2415. (j) Morao, I.; Lecea, B.; Cossió, F. P. *J. Org. Chem.* **1997**, *62*, 7033. (k) Domingo, L. R.; Arnó, M.; Andrés, J. *J. Am. Chem. Soc.* **1998**, *120*, 1617. (l) Domingo, L. R.; Picher, M. T.; Zaragozá, R. J. *J. Org. Chem.* **1998**, *63*, 9183.

(11) (a) Becke, A. D. *J. Chem. Phys.* **1993**, *98*, 5648. (b) Lee, C.; Yang, W.; Parr, R. G. *Phys. Rev. B* **1988**, *37*, 785.

(12) Hehre, W. J.; Radom, L.; Schleyer, P. v. R.; Pople, J. A. *Ab Initio Molecular Orbital Theory*; Wiley: New York, 1986.

(13) (a) Schlegel, H. B. *J. Comput. Chem.* **1982**, *3*, 214. (b) Schlegel, H. B. Geometry Optimization on Potential Energy Surface. In *Modern Electronic Structure Theory*; Yarkony D. R., Ed.; World Scientific Publishing: Singapore, 1994.

(14) (a) McIver, J. W. J.; Komornicki, A. *J. Am. Chem. Soc.* **1972**, *94*, 2625. (b) McIver, J. W. J. *Acc. Chem. Res.* **1974**, *7*, 72.

(15) (a) Schwenke, D. W.; Truhlar, D. G. *J. Chem. Phys.* **1985**, *82*, 2418. (b) Frisch, M. J.; Del Bene, J. E.; Binkley, J. S.; Schaefer, H. F., III, *J. Chem. Phys.* **1986**, *84*, 2279.

(16) (a) Reed, A. E.; Weinstock, R. B.; Weinhold, F. *J. Chem. Phys.* **1985**, *83*, 735. (b) Reed, A. E.; Curtiss, L. A.; Weinhold, F. *Chem. Rev.* **1988**, *88*, 899.

(17) Frisch, M. J.; Trucks, G. W.; Schlegel, H. B.; Gill, P. M. W.; Johnson, B. G.; Robb, M. A.; Cheeseman, J. R.; Keith, T.; Petersson, G. A.; Montgomery, J. A.; Raghavachari, K.; Al-Laham, M. A.; Zakrzewski, V. G.; Ortiz, J. V.; Foresman, J. B.; Cioslowski, J.; Stefanov, B. B.; Nanayakkara, A.; Challacombe, M.; Peng, C. Y.; Ayala, P. Y.; Chen, W.; Wong, M. W.; Andres, J. L.; Replogle, E. S.; Gomperts, R.; Martin, R. L.; Fox, D. J.; Binkley, J. S.; Defrees, D. J.; Baker, J.; Stewart, J. P.; Head-Gordon, M.; Gonzalez, C.; Pople, J. A. *Gaussian 94*; Gaussian, Inc.: Pittsburgh, PA, 1995.

**Scheme 3**

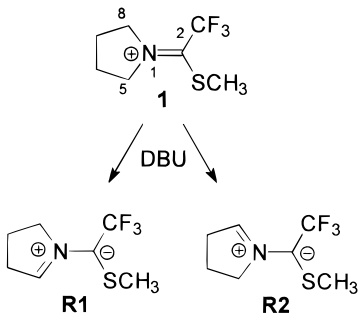


**Scheme 4**

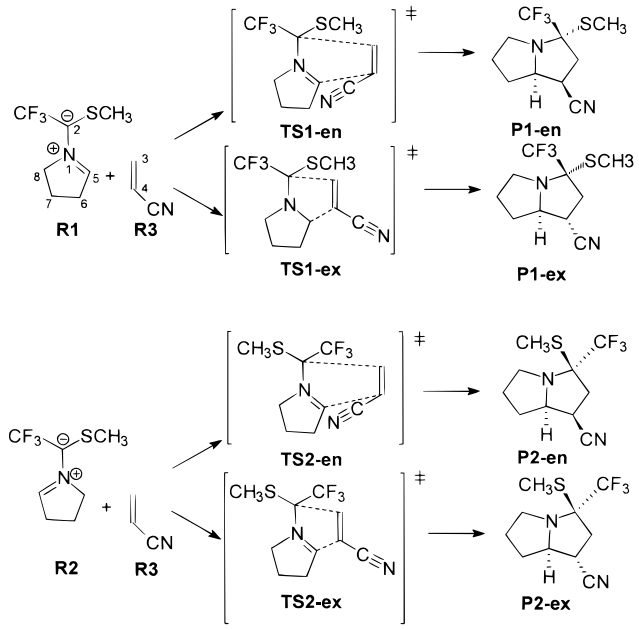


abstraction of the amidium cation **1**, using DBU (1,8-diazabicyclo[5.4.0]undec-7-ene) as base.[3] The presence of the two electron-withdrawing groups facilitates the deprotonation process. However, the presence of two nonequivalent methylenes in the amidium cation **1**, due to the restricted rotation around the N1−C2 bond, and the presence of the neighboring $-CF_3$ and $-SCH_3$ substituents allow the formation of two isomer azomethine ylides, **R1** and **R2** (see Scheme 3).

A stereochemical analysis of the cycloadducts reported by Viehe et al.[3] points out that the two diastereomer cycloadducts **P1-en** and **P2-en** come from **R1** and **R2**, respectively (see Scheme 4). Consequently, the two isomer ylides must be in the reaction mixture. Thus, previous to studying the 1,3-DC reaction, the geometries of these azomethine ylides were optimized in order to know their electronic structures.

Figure 2 presents the geometries of the ylides **R1** and **R2** including several electronic and structural parameters, while the total energies are given in Table 1. The ylide **R1** is slightly more stable than **R2** (0.3 kcal/mol). Although most of the cycloadduct is obtained from the more stable ylide **R1**, this small relative energy does not account for the diastereoselectivity observed (95:5). The relative stability between **R1** and **R2** can be rationalized by the different steric hindrance that appears between the azomethine hydrogens, H5 and H8, and the neighboring $-SCH_3$ and $-CF_3$ groups, respectively, which is larger for **R2** (see Figure 2).

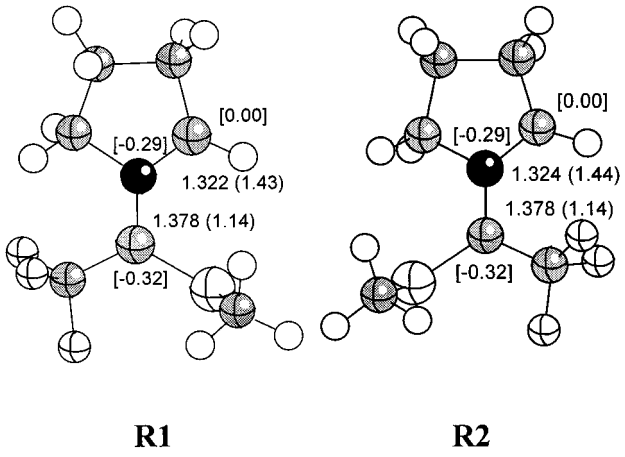


**Figure 2.** B3LYP/6-31G* optimized geometries of the azomethine ylides **R1** and **R2**. The bond lengths are given in angstroms. Values in ( ) correspond to the Wiberg bond order, while those in [ ] correspond to the natural charges.

**Table 1. Total Energies (au) and Relative Energies[a] (kcal/mol, in Parentheses) for the Stationary Points of the Reaction between the Azomethine Ylides R1 and R2 and Acronitrile R3**

| | B3LYP/6-31G* | | B3LYP/6-31+G** | |
|---|---|---|---|---|
| **R1** | −1025.175 874 | | −1025.223 107 | |
| **R3** | −170.831 551 | | −170.845 001 | |
| **CM1-en** | −1196.016 450 | (−3.0[c]) | −1196.072 363 | (−2.5[c]) |
| **CM1-ex** | −1196.011 727 | (−1.1[c]) | −1196.070 148 | (−1.2[c]) |
| **TS1-en** | −1196.010 761 | (−2.1) | −1196.066 082 | (1.3) |
| **TS1-ex** | −1196.005 218 | (1.4) | −1196.061 181 | (4.4) |
| **P1-en** | −1196.083 897 | (−48.0) | | |
| **P1-ex** | −1196.086 648 | (−49.7) | | |
| **R2** | −1025.175 447 | (0.3[b]) | −1025.222 646 | (0.3[b]) |
| **CM2-en** | −1196.014 025 | (−2.7[c]) | −1196.072 516 | (−2.9[c]) |
| **CM2-ex** | −1196.011 257 | (−1.3[c]) | −1196.069 275 | (−0.8[c]) |
| **TS2-en** | −1196.009 186 | (−1.4) | −1196.064 568 | (1.9) |
| **TS2-ex** | −1196.003 886 | (2.0) | −1196.059 522 | (5.1) |
| **P2-en** | −1196.084 326 | (−48.5) | | |
| **P2-ex** | −1196.087 877 | (−50.8) | | |

[a] Relative to **R1**+**R3** or **R2**+**R3**. [b] Relative to **R1**. [c] BSSE correction included.

The N1−C2 and N1−C5 bond lengths for the two azomethine ylides are 1.38 and 1.32 Å, respectively. Although these bond lengths are similar, the bond order analysis[18] shows that the N1−C2 bond (1.14 BO) has more single-bond character than the N1−C5 one (1.43 BO). The natural population analysis for these 2-azaallyl anion systems indicates that the negative charge is located mainly in the N1 and C2 centers, the latter being the center that supports more negative charge. This dissymmetric charge distribution is due to a strong polarization of the 2-azaallyl anion because of the presence of two electron-withdrawing groups at C2. Consequently, the C2 carbon atom is the most nucleophilic center of these azomethine ylides.

**II. 1,3-DC Reaction of the Azomethine Ylides R1 and R2 with Acronitrile R3. (i) Energies.** For each one of the azomethine ylides **R1** and **R2**, there are four reactive channels corresponding to the *endo* and *exo* approach of the polarophile **R3** in two regioisomer possibilities. However, a preliminary HF/3-21G study of the PES allows us to discard the regioisomer channels along C3−C5 and C2−C4 bond formation processes,

(18) Wiberg, K. B. *Tetrahedron* **1968**, *24*, 1083.

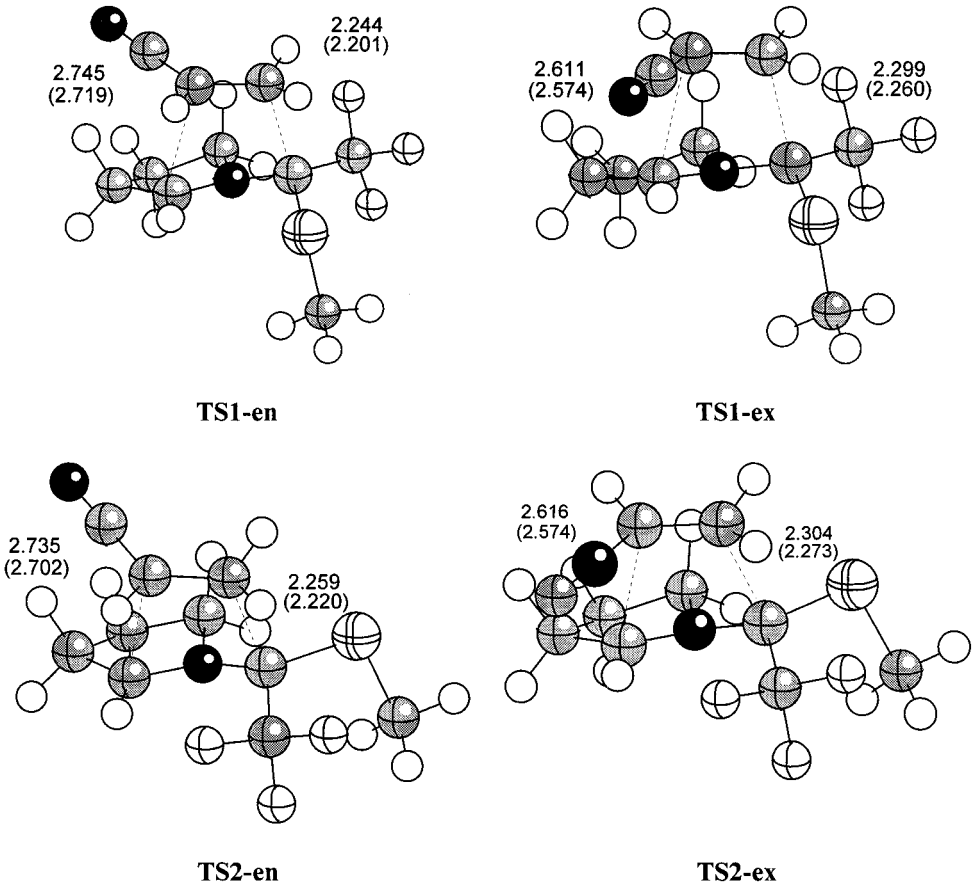


**Figure 3.** Selected geometrical parameters for transition structures corresponding to the 1,3-DC reaction between the azomethine ylides **R1** and **R2** and acronitrile **R3**. The values of the lengths of the C−C bonds directly involved in the reaction obtained at B3LYP/6-31G* and B3LYP/6-31+G** ( ) are given in angstroms.

because they are very energetic. This result is in agreement with the strong dissymmetric charge distribution found for these ylides and accounts for the total regioselectivity observed. Consequently, we have studied four TSs, **TS1-en**, **TS1-ex**, **TS2-en**, and **TS2-ex**, corresponding to the *endo* and *exo* approach of the polarophile **R3** to the dipoles **R1** and **R2**, respectively, with formation of the C2−C3 and C4−C5 single bonds.

A schematic representation of the stationary points along the *endo*/*exo* attacks of dipolarophile **R3** to the dipoles **R1** and **R2** is presented in Scheme 4. The geometries of the TSs are displayed in Figure 3, while Table 1 reports the values of total and relative energies for the stationary points along the different reactive channels. In Figure 4 a schematic representation of the energy profiles for the different reaction pathways is depicted.

In addition, the **TS3** corresponding to the 1,3-DC of **R1** with ethene has been also studied to establish the substituent effects on the dipolarophile. Figure 5 displays the geometry of this TS.

From these TSs the related minima associated with the final cycloadducts can be obtained, **P1-en**, **P1-ex**, **P2-en,** and **P2-ex**. All cycloadditions are very exothermic processes, in the range of −48.0 to −50.8 kcal/mol, the *exo* cycloadducts (**P1-ex** and **P2-ex**) being slightly more stable than the *endo* ones (**P1-en** and **P2-en**). The cycloadduct **P1-en** is the majority product (96%), whereas the **P2-en** is the minority (4%); the cycloadducts **P1-ex** and **P2-ex** have not been observed. The experimental results indicate that this 1,3-DC reaction takes place with

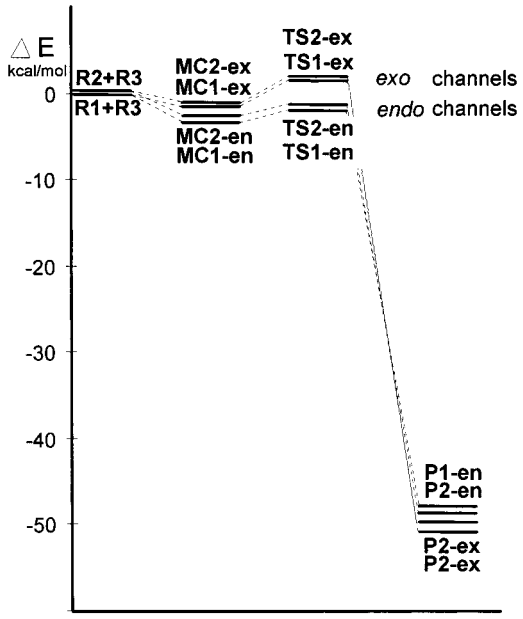


**Figure 4.** Schematic representation of the different energy profiles for the 1,3-DC reaction between the azomethide ylides **R1** and **R2** and acronitrile **R3**.

a total regio- and stereoselectivity, due to the fact that the two diastereomeric cycloadducts arise from the two isomer dipoles **R1** and **R2**, via the more favorable *endo* reactive channels (see Scheme 4).

An exhaustive exploration of the PES allows us to find several molecular complexes (MC) associated with very

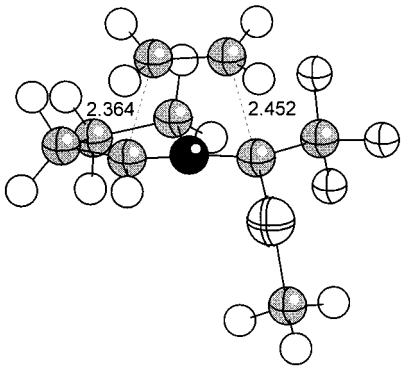


**Figure 5.** B3LYP/6-31G* transition structure **TS3** for the 1,3-DC reaction between azomethine ylide **R1** and ethene.

early stages of the 1,3-DC reactions and situated on a very flat region that controls the access to the different reactive channels. The MC formations may take place in different arrangements of the reactants, with a larger distance of the dipole and dipolarophile which corresponds to different van der Waals complexes.[19] Thus, four MCs have been studied, **MC1-en**, **MC1-ex**, **MC2-en**, and **MC2-ex**, which are associated with the four reactive channels. In these MCs, both dipole and dipolarophile fragments are in a parallel disposal, the distances between the two fragments being ca. 4−5 Å. It is possible to relate the geometry of the MCs to the geometry of TSs and cycloadducts along the different reactive channels. These MCs are more stable than the isolated reactants **R1** + **R3** and **R2** + **R3**, in the range 1.1−3.0 kcal/mol, the *endo* MCs (ca. 1.9 and 1.4 kcal/mol) being more stable than the *exo* ones.

The 6-31G* potential energy barriers for the most favorable *endo* TSs, **TS1-en** and **TS2-en**, have negative values (−2.1 and −1.4 kcal/mol, respectively). However, if we consider the formation of the molecular complexes **MC1-en** and **MC2-en**, these barriers become positive (0.9 and 0.6 kcal/mol, respectively). Moreover, after inclusion of diffuse functions at the 6-31+G** level the barriers for **TS1-en** and **TS2-en** relative to reactants become positive. This fact is due to a larger stabilization of dipoles **R1** and **R2** than TSs, because of a larger localization of negative charge in the former, and a decreasing of the BSSE in the TSs with the inclusion of diffuse functions (BSSEs at the 6-31G* *endo* TSs, **TS1-en** and **TS2-en**, have been estimated at 4.2 and 4.4 kcal/mol, respectively). However, the similar relative energies found at the 6-31G* and 6-31+G** levels show that both computational levels give the same stereochemical outcome.

The analysis of the potential energy barriers for the TSs relative to reactants (see Table 1) reveals that the *endo* approach is favored over the *exo* attack mode; **TS1-en** and **TS2-en** are more stable than **TS1-ex** and **TS2-ex**, in the range of 3.5 and 4.3 kcal/mol, respectively. These results are in agreement with the total *endo* stereoselectivity found experimentally.[3] Moreover, the *endo* attack to dipole **R1** is 1.0 kcal/mol more favorable than for the dipole **R2**. If we consider the formation of **R1** and **R2** as a reversible process,[20] the Curtin−Hammett principle[21] can be operative, and consequently,

(19) (a) Sustmann, R.; Sicking, W. *J. Am. Chem. Soc.* **1996**, *118*, 12562. (b) Suarez, D.; Sordo, J. A. *Chem. Commun.* **1998**, 385.

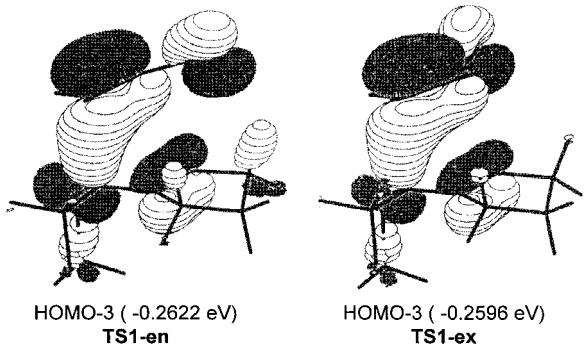


**Figure 6.** HOMOs-3 of **TS1-en** and **TS1-ex**. The drawing corresponding to **TS1-en** shows the delocalization across the axial H6 hydrogen.

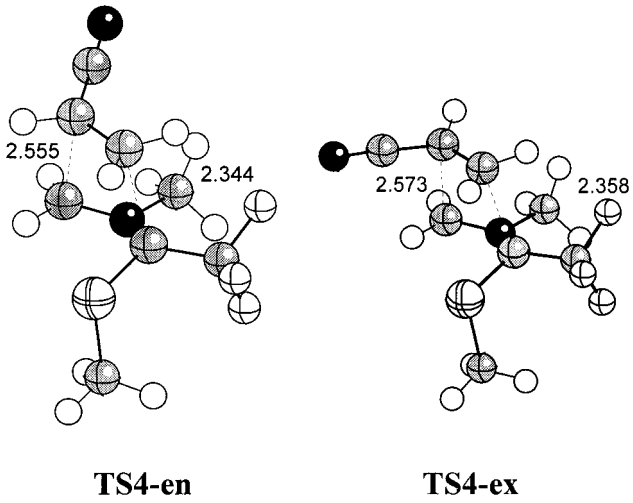


**Figure 7.** *Endo* and *exo* transition structures corresponding to the 1,3-DC reaction between the azomethine ylide **3** and acronitrile **R3**.

the relative energy of **TS1-en** and **TS2-en** allows us to explain the diastereoselectivity observed (at −78 °C, a 96:4 ratio corresponds to an energetic difference of ca. 1.1−1.2 kcal/mol).

An analysis of molecular orbitals for **TS1-en** and **TS1-ex** allows us to explain the origin of the *endo* selectivity. The more relevant molecular orbitals HOMO and HOMO-3, which are associated mainly with the two $\sigma$-bonds being formed, are also delocalized along the electron-withdrawing −CN group belonging to the dipolarophile fragment (see Figure 6). For the *endo* approaches there is a hyperconjugative delocalization along the −CN group and the neighboring axial H6 hydrogen at **TS1-en**, which allows an increase of the electronic delocalization on aforementioned molecular orbitals (see Figure 6). As a consequence, when we studied the 1,3-DC reaction between acronitrile and the azomethine **3**, without the C6 methylene (see Figure 7), the *endo* **TS4-en** is only 1.2 kcal/mol more stable than the *exo* **TS4-ex**, allowing the evaluation of this hyperconjugative effect of ca. 2.3 kcal/mol.

(20) The deprotonation processes of the amidium cation **1** with DBU to give **R1** and **R2** have been studied at the HF/6-31G* level. The two competitive reactive channels present TSs with similar energies (less than 0.1 kcal/mol). This result disagrees with the stereochemical outcome if an irreversible acid−base process is considered.

(21) (a) Curtin, D. Y. *Recl. Chem. Prog.* **1954**, *14*, 111. (b) Hammett, L. P. *Physical Organic Chemistry*; McGraw-Hill: New York, 1970.

**Table 2. Activation Enthalpies (in kcal/mol), Entropies (in kcal/(mol·K)), and Gibbs Energies (in kcal/mol) Computed at −78 °C and 1 Atm for the Reaction between the Azomethine Ylides R1 and R2 and Acronitrile R3**

| | $\Delta H^{\ddagger}$ | $\Delta S^{\ddagger}$ | $\Delta G^{\ddagger}$ |
|---|---|---|---|
| **TS1-en** | 2.2 | −48.3 | 11.8 |
| **TS1-ex** | 5.1 | −46.4 | 14.3 |
| **TS2-en** | 2.8 | −48.2 | 12.3 |
| **TS2-ex** | 6.0 | −47.1 | 15.3 |

Finally, the values of activation enthalpies, entropies, and Gibbs energies corresponding to the four reactive channels have been estimated by means of the potential energy barriers computed at the B3LYP/6-31+G** level along with the B3LYP/6-31G* harmonic frequencies. These frequencies have been scaled by 0.98. The activation Gibbs energies have been computed at −78 °C, which is the experimental temperature for the 1,3-DC reaction.[3] The enthalpy and entropy changes were calculated from standard statistical thermodynamic formulas.[12,22]

The results are summarized in Table 2. The inclusion of the zero-point energy and of thermal contributions to the potential energy barriers leads to a small decrease in the relative energy between the *endo* and *exo* TSs. Moreover, the activation entropies corresponding to the *endo* approaches are slightly more negative than those corresponding to the *exo* ones. As a consequence, the differences between the *endo*/*exo* activation Gibbs energies (2.5 and 3.0 kcal/mol, for **R1** and **R2**, respectively) are lower than the ones corresponding to the potential energy barriers (3.1 and 3.2 kcal/mol, for **R1** and **R2**, respectively). The favorable orbital interactions that appear along the *endo* approach are responsible for the slightly more negative activation entropies for the *endo* TSs than the *exo* ones (1.9 and 1.1 cal/(mol·K), for **R1** and **R2**, respectively). As for the Diels−Alder reactions, these activation entropies are very negative (in the range −46.4 to −48.3 cal/(mol·K)), and they are responsible for the fact that the activation Gibbs energy for the more favorable reactive channel increases to 11.8 kcal/mol. This low activation Gibbs energy is in agreement with the low temperature used for this 1,3-DC reaction (−78 °C).[3]

**(ii) Geometrical Parameters.** A comparison of the geometrical parameters obtained at two computational levels shows no significant differences (see Figure 3). The C4−C5 bond lengths are larger than the C2−C3 ones, showing a high dissymmetry for the two carbon−carbon bonds being formed at these TSs. The asynchronicities measured as the difference between the values of both bonds being formed, $\Delta r = d(\text{C4}-\text{C5}) - d(\text{C2}-\text{C3})$, are in the range 0.3−0.5 Å, being larger for the *endo* TSs than for the *exo* ones.

For the **TS3**, the lengths of the two carbon−carbon bonds being formed are 2.364 and 2.452 Å, showing a more synchronous cycloaddition process, $\Delta r = 0.1$ (see Figure 5). These large bond distances are similar to those found by Annunziata et al. for the 1,3-DC reaction of the azomethine ylide **2** with ethylene (see Figure 1), indicating that these TSs are remarkably early.[5]

The presence of the electron-withdrawing −CN group in the dipolarophile increases the dissymmetry of the two bonds being formed in the four TSs. The bond being formed α to the nitrile group is longer than that $\beta$ to this group. For this dipolarophile the $\beta$ carbon is more electrophilic than the α one, while for dipole the C2-substituted position is more nucleophilic. Consequently, there is more bond formation and a shorter bond length at the $\beta$ carbons in the TSs. However, the mean of the two bonds being formed for these dissymmetric TSs, ca. 2.4 Å, is similar to those found at **TS3**, indicating that these four TSs are also remarkably early.

**Table 3. B3LYP/6-31G* Imaginary Frequency ($cm^{-1}$), Hessian Unique Negative Eigenvalue (au), Main Components of the Transition Vector (au), and Corresponding Geometric Parameters (Lengths in Å, Angles in deg) for the Transition Structures Corresponding to the Reaction between the Azomethine Ylides R1 and R2 and Acronitrile R3**

| | **TS1-en** | | **TS1-ex** | |
|---|---|---|---|---|
| imaginary frecuency | 216.9i | | 236.6i | |
| eigenvalue | −0.01144 | | −0.01246 | |
| C2−C3 | 0.758 | 2.244 | 0.721 | 2.299 |
| C4−C5 | 0.439 | 2.745 | 0.492 | 2.611 |
| C2−C3−H3a | −0.139 | 92.5 | −0.146 | 91.1 |
| C2−C3−H3b | −0.148 | 93.3 | −0.135 | 93.5 |
| C5−N1−C2−S | −0.207 | 38.4 | −0.203 | 42.2 |
| C2−N1−C5−C4 | 0.127 | 55.2 | 0.121 | 56.6 |
| C8−N1−C2−C5 | 0.130 | 159.9 | 0.135 | 158.6 |
| C2−N1−C5−H5 | 0.181 | −19.6 | 0.216 | −22.4 |
| | **TS2-en** | | **TS2-ex** | |
| imaginary frequency | 212.9i | | 228.8i | |
| eigenvalue | −0.01073 | | −0.01117 | |
| C2−C3 | 0.744 | 2.259 | 0.719 | 2.304 |
| C4−C5 | 0.449 | 2.735 | 0.500 | 2.616 |
| C2−C3−H3a | −0.122 | 92.9 | −0.130 | 91.4 |
| C2−C3−H3b | −0.152 | 92.1 | −0.141 | 92.6 |
| C8−N1−C2−C6 | −0.218 | 43.4 | −0.198 | 46.8 |
| C2−N1−C5−C4 | 0.132 | 53.7 | 0.117 | 54.9 |
| C5−N1−C2−C8 | 0.142 | 157.6 | 0.137 | 156.4 |
| C2−N1−C8−H8 | 0.198 | −21.7 | 0.212 | −24.3 |

The $-CF_3$ and $-SCH_3$ substituents on the dipole fragment present a very similar disposal at these TSs. Both are in an anti conformation relative to the C2−C3 bond being formed (see Figure 3). The arrangement of the $-CF_3$ group at the TSs is twisted relative to its position in the dipoles; this increases the steric hindrance between the H8 azomethine hydrogen and the $-CF_3$ group in **TS2-en** relative to that in **R2** (the distance between the H8 hydrogen atom and the neighboring fluorine atom in **TS2-en** is 2.127 Å, whereas in **R2** it is 2.402 Å). As a consequence, **TS2-en** is 1.0 kcal/mol more energetic that **TS1-en**, whereas the difference between **R1** and **R2** is only 0.3 kcal/mol.

**(iii) Transition Vectors and Analysis of Frequencies.** In Table 3, the imaginary frequency and the main TV components and their corresponding geometric parameters are reported for the four TSs. The TVs for these TSs are very similar. The dominant TV components are associated with the C2−C3 and C4−C5 bond distances, which correspond to the two carbon−carbon single bonds that are being formed along the 1,3-DC process. The values of the C2−C3 components, in the range 0.72−0.76, are larger than for the C4−C5 ones, in the range 0.44−0.50, showing also the asynchronicity of the process.

Several bond angles and dihedral angles participate also in the TV. The C2−C3−H3a and C2−C3−H3b components are associated with the hybridization change that is developing in the C3 center from $sp^2$ to $sp^3$, while the different dihedral angles are also associated with the

(22) Jorgensen, W. L.; Lim, D.; Blake, J. F. *J. Am. Chem. Soc.* **1993**, *115*, 2936.

**Table 4. Wiberg Bond Orders at the Transition Structures TS1-en, TS1-ex, TS2-en, and TS2-ex**

| | TS1-en | TS1-ex | TS2-en | TS2-ex |
|---|---|---|---|---|
| N1−C2 | 1.08 | 1.09 | 1.08 | 1.08 |
| C2−C3 | 0.35 | 0.33 | 0.34 | 0.32 |
| C3−C4 | 1.54 | 1.56 | 1.55 | 1.56 |
| C4−C5 | 0.16 | 0.19 | 0.16 | 0.19 |
| N1−C5 | 1.40 | 1.38 | 1.39 | 1.38 |

hybridization change that is developing in the N1 center from $sp^2$ to $sp^3$.

The imaginary frequency values for the *endo* TSs, **TS1-en** and **TS2-en**, 217i and 213i $cm^{-1}$, respectively, are slightly lower that for the *exo* ones, **TS1-ex** and **TS2-ex**, these being in the range of 237i and 229i $cm^{-1}$. These low values indicate that these processes are associated with heavy atom motions, and they are lower than those for the Diels−Alder cycloadditions (ca. 500i $cm^{-1}$). These results are related to the earlier TSs found for these 1,3-DC reactions, since they have lower force constants for the two bonds being formed.

**(iv) Bond Order and Charge Analysis.** A more balanced measure of the extent of bond formation or bond breaking along a reaction pathway is provided by the concept of bond order (BO). This theoretical tool has been used to study the molecular mechanism of chemical reactions.[23] To follow the nature of the these processes, the Wiberg bond indices[18] have been computed by using the NBO analysis as implemented in Gaussian94. The results are included in Table 4.

The BO analysis of these TSs also shows the asynchronicity of the bond formation process along the four reactives channel. The BOs for C2−C3 bonds being formed have larger values than for the C4−C5 ones. Moreover, the C2−C3 BOs, in the range 0.35−0.32, are smaller than those for the TSs of Diels−Alder cycloadditions (ca. 0.5), showing that these 1,3-DC reactions are early processes.

The similar BOs for the two carbon−carbon bonds being formed for **TS3**, 0.26 and 0.29, show a more synchronous bond formation process for the 1,3-DC reaction between the azomethine ylide **R1** and ethene and that the **TS3** is remarkably early.

A comparison of the results presented in Table 1 with those in Table 4 indicates a relation between the relative energies of the four TSs and the asynchronicity of the processes. The less energetic *endo* TSs are slightly more asynchronous than the *exo* ones; a similar relation can be seen between the TSs for **R1** and **R2** channels. This fact supports the empirical role that holds for a variety of Diels−Alder cycloadditions that "for dissymmetrically substituted dienophiles, the more asynchronous TS has the lower energy".[10i,22,24]

The natural population analysis for these TSs gives a small charge transfer for these processes, being slightly larger for the *endo* TSs (0.23e) than for the *exo* ones (0.20e). This low charge transfer found for these 1,3-DC reactions can be related with the presence of the two electron-withdrawing groups in the dipole, which prevents the charge transfer process. Moreover, the larger charge-transfer found along the *endo* approach than along the *exo* one (0.03 e) can be related with the hyperconjugative delocalization found for the *endo* TSs, which increase the electron-withdrawing character of the −CN group. These facts can be associated with the asynchronicity of the process. A larger charge-transfer process gives a more asynchronous TS, with a lower energy.

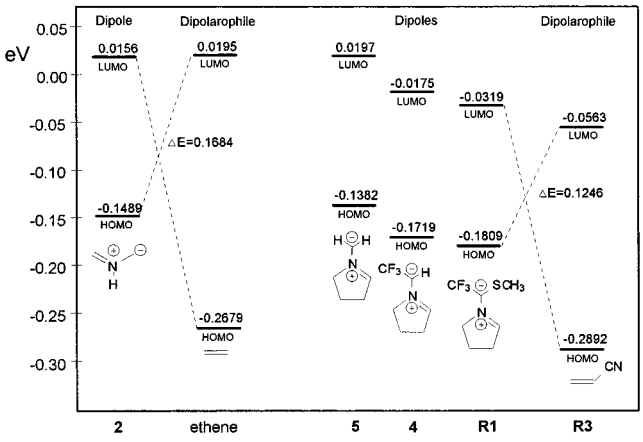


**Figure 8.** Frontier molecular orbital (B3LYP/6-31G*) interactions in the 1,3-DC reactions between the azomethine ylide **2** + ethene and the azomethine ylide **R1** + acronitrile **R3**. The FMO of the azomethine ylides **4** and **5** are also included.

**(v) Frontier Molecular Orbital Analysis.** These 1,3-DC reactions appear to be under frontier control, the FMO model being capable of explaining the substituent effects for these reactions. In Figure 8, the FMO analysis for the reactions between azomethine ylide **2** + ethene and azomethine ylide **R1** + acronitrile **R3** is presented. The main HOMO−LUMO interaction for both reactions occurs between the HOMO of the dipole ($HOMO_{dipole}$) and the LUMO of the dipolarophile ($LUMO_{dipolarophile}$).

The $HOMO_{dipole}$ of azomethine ylide **2** is quite raised in energy, and this approach at first seems reasonable. However, the HOMO of the azomethine ylide **R1** (−0.1809 eV) is lower than that for the former (−0.1489 eV), because of the presence of both substituents on **R1**. This fact increases the gap of the more relevant ($HOMO_{dipole}$)−($LUMO_{dipolarophile}$) energy separation and consequently increases the activation energy of the **R1** + ethene reaction. However, the presence of the electron-withdrawing −CN group in the dipolarophile **R3** decreases more effectively the $LUMO_{dipolarophile}$ energy, and consequently there is an effective decreasing of the gap for the more relevant ($HOMO_{dipole}$)−($LUMO_{dipolarophile}$) energy separation, lowering the activation energy for the reaction between **R1** and **R3**.

An analysis of the HOMO energies for the azomethine ylides **R1**, **4** (**R1** without the $-SCH_3$ group), and **5** (**R1** without any substituent) allows us to assess the electron-withdrawing character of these groups, which stabilizes the corresponding MO relative to the nonsubstituted azomethine ylide **5** (see Figure 8). Moreover, the larger stabilization of the HOMO of **4** than that of **R1** allows also to assess the $-CF_3$ as the most electron-withdrawing group.

The regioselectivity can be also rationalized in terms of FMO interactions. The essential difference between the regioisomer reaction pathways concerns the relative orientation of the two asymmetric fragments (dipole and

(23) (a) Varandas, A. J. C.; Formosinho, S. J. F. *J. Chem. Soc., Faraday Trans. 2* **1986**, 282. (b) Lendvay, G. *THEOCHEM* **1988**, *167*, 331. (c) Lendvay, G. *J. Phys. Chem.* **1989**, *93*, 4422. (d) Lendvay, G. *J. Phys. Chem.* **1994**, *98*, 6098.

(24) Froese, R. D. J.; Organ, M. G.; Goddard, J. D.; Stack, T. D. P.; Trost, B. M. *J. Am. Chem. Soc.* **1995**, *117*, 10931.

dipolarophile). Along the more favorable regioisomer pathways, there is an optimized overlap between the HOMO of the dipole fragment (associated with the $\pi$ system of the substituted azomethine ylide) and the LUMO of the dipolarophile fragment (associated with $\pi^*$ system of acronitrile). This is due to the biggest molecular orbital coefficients at the C2 and C3 atoms in these FMOs. This fact justifies the total regioselectivity found in this 1,3-DC reaction, and it can be rationalized by a stronger polarization of the azomethine ylide system due to the presence of the two electron-withdrawing groups in the azomethines ylides **R1** and **R2**.

## Conclusions

In the present work we have carried out a theoretical study of the molecular mechanism for the 1,3-DC reactions of two isomer trifluoromethyl thiomethyl azomethine ylides with acronitrile using density functional theory methods with the B3LYP functional and the 6-31G* and 6-31+G** basis sets. The PES has been explored and four reactive pathways have been characterized by means of the localization of the corresponding stationary points. Relative rates, regioselectivity, and *endo* stereoselectivity have been analyzed and discussed as a function of the substituents on dipole and dipolarophile fragments.

For these 1,3-DC reactions, DFT calculations give one-step cycloaddition processes via dissymmetric transition structures, which can be associated with pericyclic processes. Although the presence of the two electron-withdrawing groups in the dipole can increase the potential energy barrier for these cycloadditions, the presence of a more effective electron-withdrawing −CN group in the dipolarophile favors these 1,3-DC reactions. These reactions present a total regioselectivity and *endo* stereoselectivity, due to a strong polarization of both dissymmetric dipole and dipolarophile reactants, and a favorable hyperconjugative delocalization that appears along the *endo* approach, which favor the charge-transfer process. Moreover, the presence of the two substituents on azomethine ylide ($-CF_3$ and $-SCH_3$) are responsible for the high diastereoselectivity found experimentally. The full agreement between this DFT study at the B3LYP/6-31G* theory level and the experimental results allows us to extend this computational approach to the study of this sort of 1,3-DC reaction.

**Acknowledgment.** This work was supported by research funds provided by the Universidad de Valencia (Project UV97-2219) and by the Conselleria de Cultura Educació i Ciéncia, Generalitat Valenciana (Project GV97-CB11-96). I thank Professor I. Nebot-Gil for helpful comments. All calculations were performed on a Cray-Silicon Graphics Origin 2000 with 64 processors of the Servicio de Informática de la Universidad de Valencia. I am most indebted to this center for providing us with computer capabilities.

JO9822683